Available online at www.sciencedirect.com
ScienceDirect
Physica A 387 (2008) 457–466
PHYSICA A
www.elsevier.com/locate/physa

Local inhomogeneity in two-lane asymmetric simple exclusion processes coupled with Langmuir kinetics

Ruili Wang[a,*], Mingzhe Liu[a], Rui Jiang[b]

[a] *Institute of Information Sciences and Technology, Massey University, New Zealand*
[b] *School of Engineering Science, University of Science and Technology of China, Hefei 230026, China*

Received 2 May 2007; received in revised form 5 July 2007
Available online 4 October 2007

Abstract

The effects of local inhomogeneity in a two-lane asymmetric simple exclusion process coupled with Langmuir kinetics are studied. The model is related to some biological processes such as the movement of molecular motors on parallel homogeneous and inhomogeneous filaments without restrictions for them to jump between these protofilaments as well as random motors (e.g., kinesin) attachments to and detachments from filaments. The local inhomogeneity is assumed to be located at one of the two lanes. The effects of such inhomogeneity on its neighboring lane are focused in this paper. Density and inter-lane current are investigated. It is found that when the value of the hopping rate (p) is small, the local inhomogeneity effect can be observed on both lanes due to particles changing lanes. The effect is weakened when either p and/or lane-changing rate (Ω) increases. Average density and average current of the two lanes are also calculated, and it is found that the average density profile exhibits a complex variation behavior with the increase of Ω when p, Ω_A (attachment rate) and Ω_D (detachment rate) are small. Mean-field approximation is presented and it agrees well with our Monte Carlo simulations.

Keywords: Local inhomogeneity; Two-lane TASEPs; Langmuir kinetics

1. Introduction

Non-equilibrium intracellular transport phenomena have been analyzed and modeled from the viewpoint of statistical physics since early 1970s. The main issues of modeling molecular motor traffic may include (i) how to properly describe the movement of motor proteins and interactions between them at a microscopic level; and (ii) how to obtain the macroscopic traffic properties by analyzing molecular traffic phases and phase transitions. Efforts to understand these collective dynamics of molecular motors may be expected to disclose the cause of motor-related diseases (e.g, in Ref. [1], and references therein) and to assist in appropriate control and cure measurements.

Totally asymmetric simple exclusion processes (TASEPs) play a primary role in the study of non-equilibrium systems [2] and have been widely used to describe stochastic dynamics of multi-particle interactions in chemistry and physics [3,4]. TASEPs are non-equilibrium one-dimensional lattice models in which particles update their states through hard-core exclusion and move unidirectionally. An extension of a single-lane TASEP, incorporating Langmuir

* Corresponding author. Tel.: +64 6 3569099 2548; fax: +64 6 3502259.
E-mail address: r.wang@massey.ac.nz (R. Wang).

0378-4371/$ - see front matter © 2007 Elsevier B.V. All rights reserved.
doi:10.1016/j.physa.2007.09.042

kinetics (LK, the attachment and detachment of particles), has been studied extensively [5,6]. In Ref. [5], a phase coexistence between the low-density and high-density phases is presented and a mean-field method is developed. The mean-field equation derived for the density profile has shown to agree with the Monte Carlo simulations. Their model is also referred to as the PFF model. Popkov et al. argued that the mean-field approximation cannot be used in general [6]. They believe that the coincidence with the Monte Carlo simulations in Ref. [5] is due to the lack of correlation in the true steady state of the TASEP. Furthermore, they claimed that the stationary density profile can be derived, in general, using a hydrodynamic equation developed by them [6], which can take correlations into account. They have also demonstrated the effectiveness of the equation, which can correctly describe the density profiles on a quantitative level of the Katz–Lebowitz–Spohn (KLS) model [7,8], while a mean-field approach has failed to reproduce some features of the system, e.g., phase separation into three distinct density regimes.

TASEPs have also been applied successfully in modeling particles in biological systems [5,6,9–15]. For example, experimental observations [16] have found that motor protein kinesins can move along the parallel protofilaments of microtubules without restrictions for them to jump between these protofilaments. Also, random motors (e.g., kinesins) are found to attach to and detach from filaments [17]. Based on these findings, two-lane TASEP models have been proposed and investigated [18–23].

Recently, the study on local inhomogeneity (which means the hopping rate of one (or several) lattice site of a lane is different from the hopping rates of the other sites of the lane, e.g., a lattice site may be associated with a random quenched hopping rate [24]) has received much attention [24–28]. Local inhomogeneities can be relevant to many biological processes such as energy transition of guanine triphosphate (GTP) hydrolysis [29], cell growth [30], excitation and inhibition of neurons [31], and respiratory infection [32]. For example, a local inhomogeneity of immunoreactivity may lead to a high susceptibility to respiratory infection [32]. Understanding the mechanism of interruption of intracellular transport is expected to shed light on exploring the causes of the diseases related to congestion or local inhomogeneity, as shown in Refs. [29–32], and possibly helping to prevent, diagnose, control and cure the diseases.

Models proposed in Refs. [24–28] investigated the effects of local inhomogeneity on TASEPs coupled with/without Langmuir kinetics (LK) in a single-lane system. A novel phase, *bottleneck phase*, is introduced in Ref. [24] to describe the current independently of boundary conditions. Due to the bottleneck phase, several rich bottleneck-induced mixed phases are reported.

Filaments that protein motors move on are similar to parallel multi-lanes. Thus, using a two- or multi-lane system to simulate the traffic of molecular motors can provide a more realistic description of molecular motor traffic. It is possible that the inhomogeneity occurs only on one lane. Therefore, it is important to investigate the effects of such local inhomogeneity on neighboring lanes.

This paper is focused on the effect of one lane with local inhomogeneity on its neighboring lane in a two-lane TASEP with Langmuir kinetics (LK) and lane changing between the two lanes. This has not been studied before, to the best of our knowledge. The model we describe here is inspired by the dynamics of the motor proteins, for instance, the unidirectional motion of molecular motors along filaments [33], random motors (e.g., kinesin) attachments and detachments to filaments [17], freely changing to the adjacent filaments [16] and local inhomogeneity in a filament [29]. It is expected that the study on a bottleneck of such a two-lane system can shed light on a better understanding of interacting particles in biological systems as well as other areas such as in vehicular traffic where bottlenecks (e.g., on ramps, road construction or a speed limit zone) are commonly met.

The paper is organized as follows. In Section 2, we give a description of our two-lane TASEP model, considering attachment and detachment of particles to both lanes, lane changing between the two lanes and a local inhomogeneity only on one of the two lanes. In Section 3, we present and discuss the results of the Monte Carlo simulations (MCS). In Section 4, a mean-field approximation (MFA) is obtained and the quantitative agreement between the theory and the simulation is confirmed. Finally, we give our conclusions in Section 5.

2. Model

Our model is an extension of the models introduced in Refs. [21,22,25,27,24]. The model is defined in a two-lane lattice of $N \times 2$ sites, where N is the length of a lane. Particles are assumed to move from the left to the right, as shown in Fig. 1. Site 1 and site N define the left and right boundaries respectively, while a set of sites $2, \ldots, (N-1)$ is referred to as the bulk. We assume that all sites on lane 1 are homogeneous, while site k on lane 2 is inhomogeneous and the other sites on lane 2 are homogeneous. We introduce an occupation variable $\tau_{\ell,i}$ ($\ell = 1$ or 2) where $\tau_{\ell,i} = 1$

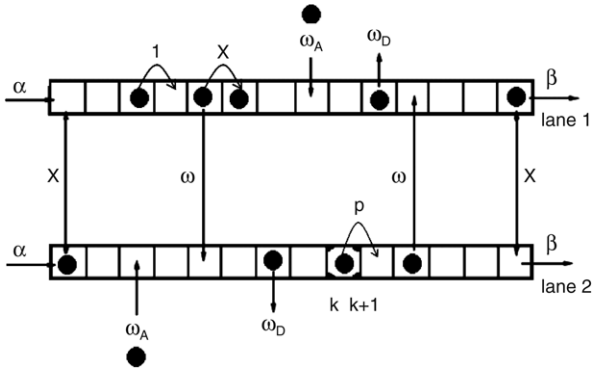

Fig. 1. The schematic representation of local inhomogeneity in a two-lane TASEP coupled with Langmuir kinetics and symmetric inter-lane transition.

(or $\tau_{\ell,i} = 0$) indicates that the state of the ith site in the ℓth lane is occupied (or vacant). We apply the following dynamical rules (also see Fig. 1). For each time step, site (ℓ, i) is chosen at random.

- $i = 1$. (i) If $\tau_{\ell,1} = 0$, a particle enters the system with probability α. (ii) If $\tau_{\ell,1} = 1$ and $\tau_{\ell,2} = 0$, the particle in site $(\ell, 1)$ moves into site $(\ell, 2)$. (iii) If $\tau_{\ell,1} = 1$ and $\tau_{\ell,2} = 1$, the particle in site $(\ell, 1)$ stays there. No lane change occurs here.[1]
- $i = N$. If $\tau_{\ell,N} = 1$, the particle leaves the system with probability β. No lane change occurs.[2]
- $1 < i < N$. (i) If $\tau_{\ell,i} = 1$, the particle may leave the system with probability ω_D. If it cannot leave the system, it moves into site $(\ell, i + 1)$ with probability p if $\tau_{\ell,i+1} = 0$. Otherwise, it changes to lane $(3 - \ell)$ with probability ω if $\tau_{3-\ell,i} = 0$. Probability p: $0 \le p < 1$ when $i = k$ and $\ell = 2$. Otherwise, $p = 1$. (ii) If $\tau_{\ell,i} = 0$, a particle enters the system with probability ω_A.

Updating rules on both lanes are illustrated in Fig. 1. For simplicity, we use a symmetric lane-changing rule. It will be the next step of our work to investigate the effects of an asymmetric lane-changing rule on the system. We use a random-sequential updating scheme, which has been widely used in the simulations of molecular motor traffic, e.g., in Refs. [5,10,11,15,18,19,22].

3. Monte Carlo simulations

In this section, the results of the Monte Carlo simulations are presented. The parameters are set to $N = 1000$, $\alpha = 0.2$, $\beta = 0.6$, $\Omega_D = 0.2$, $K = 3$ and $\Omega_A = K^*\Omega_D$.[3] Lane-changing rate Ω $(=\omega N)$ is arbitrarily given four values: 0.5, 5, 50 and 500. For simplicity, we assume that the local inhomogeneous site k is located at $k = N/2$. Thus, both the lanes can be divided into two sublanes, left sublanes and right sublanes connected by sites $N/2$ and $(N/2 + 1)$. We would like to point out when the defect is not in the middle of the lane, the phase diagram and density profile will be qualitatively the same, provided the defect is far away from the boundary. In other words, the results of the phase diagram and density profile will be qualitatively the same as that when the defect is in the middle of the lane. In simulations, stationary profiles are obtained by averaging 10^5 sampling at each site. The sampling time interval is $10N$. The first $10^5 N$ time steps are discarded to let the transient time out.

Fig. 2 shows the density $\rho(x)$ for different values of lane-changing rate Ω of both lanes with $p = 0.25$. The density $\rho(x)$ is defined as the time average of the occupation number $\tau_{\ell,i}$, and $x = i/N$. It can be seen that the local inhomogeneity of one lane can affect the other lane. From Fig. 2(a)–(d), we can also see that:

- When Ω is small, the inhomogeneity of lane 2 slightly influences density profile on lane 1. The increase of Ω increases the influence on lane 1 (see Fig. 2(a)–(d)).

[1] Our simulations show that the results remain essentially the same if lane changing is allowed on this site. This is because the densities of sites (ℓ,1) and (3-ℓ,1) are same, therefore, the lane-changing behavior will not affect the densities of the two sites.

[2] Similarly, the results remain essentially the same if lane changing is allowed on this site.

[3] As indicated in Ref. [5], in order to study the competition between bulk and boundary dynamics in large system sizes ($N \ge 1$) even $N \to \infty$, the kinetic rates are required to decrease proportionally with the system size. More precisely, we define $\Omega_A = \omega_A N$, $\Omega_D = \omega_D N$. More detailed discussions on this can be found in Ref. [6].

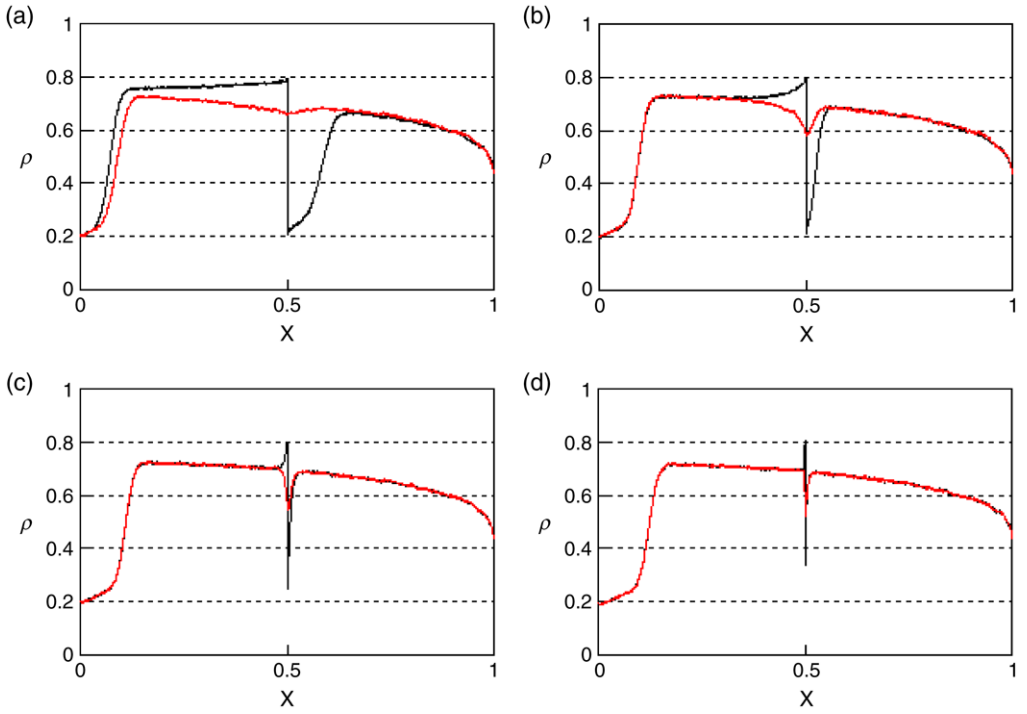

Fig. 2. (Color online) Density profiles $\rho(x)$ for different values of Ω on both lanes (red lines for lane 1 and black lines for lane 2) with $p = 0.25$. The local inhomogeneity is $x = i/N = 0.5$. (a) $\Omega = 0.5$; (b) $\Omega = 5$; (c) $\Omega = 50$ and (d) $\Omega = 500$. The system parameters are: $N = 1000$, $\Omega_A = 0.6$, $\Omega_D = 0.2$, $\alpha = 0.2$ and $\beta = 0.6$.

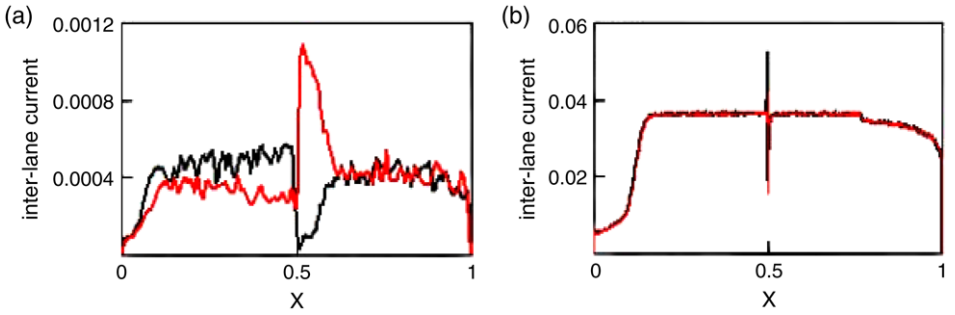

Fig. 3. (Color online) Inter-lane currents on both lanes. Red lines represent the flows from lane 1 to lane 2. Black lines represent the flows from lane 2 to lane 1. (a) $\Omega = 0.5$; (b) $\Omega = 50$. The system parameters are: $N = 1000$, $\Omega_A = 0.6$, $\Omega_D = 0.2$, $\alpha = 0.2$, $\beta = 0.6$ and $p = 0.25$.

- Density at site $N/2$ of lane 2 reaches the highest value due to local inhomogeneity (see Fig. 2(a)), while density at site $(N/2 + 1)$ is much smaller than that at site $N/2$. Furthermore, Ω has little effect on the density at site $N/2$ of lane 2 (see Fig. 2 (a)–(d)). In other words, the density at site $N/2$ of lane 2 is mainly decided by p.
- The differences of the densities between the two lanes at the same sites decrease with the increase of Ω.

In Fig. 3, one can see that the local inhomogeneity of one lane causes the different inter-lane currents in a two-lane system. This is because when a symmetric lane-change rule is adopted, the current from a high-density lane to a low-density lane is larger than the current from the low-density lane to the high-density lane. Also, comparing Fig. 3(a) to (b), we can see that when Ω increases the difference between inter-lane currents becomes smaller.

In Fig. 3(a), when $0 < x < 0.5$ (where $x = i/N$), one can see that the current (the black line in Fig. 3(a)) from lane 2 to lane 1 is larger than that from lane 1 to lane 2 (the red line in Fig. 3(a)). This is due to the bottleneck at $x = 0.5$ on lane 2 and the local inhomogeneity leads to the density wave back propagation along lane 2. Thus, density of lane 1 is smaller than that of lane 2 when $0 < x < 0.5$. When $x > 0.5$, the flow from lane 2 to lane 1 is less than

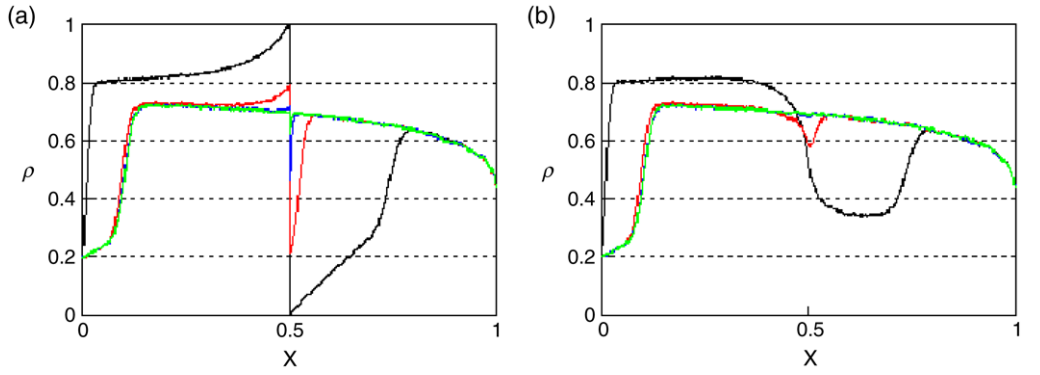

Fig. 4. (Color online) Density profiles $\rho(x)$ for different values of p. (a) for lane 2, while (b) for lane 1. $\Omega = 5$. The black lines for $p = 0$; the red lines for $p = 0.25$; the blue lines for $p = 0.5$, and the green lines for $p = 0.75$. The system parameters are: $N = 1000$, $\Omega_A = 0.6$, $\Omega_D = 0.2$, $\alpha = 0.2$ and $\beta = 0.6$.

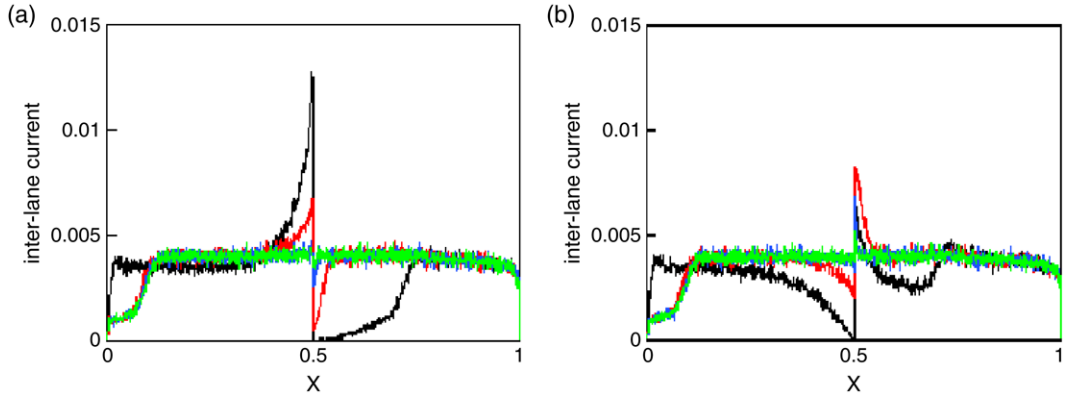

Fig. 5. (Color online) Inter-lane currents on both the lanes for different p. (a) the currents from lane 2 to lane 1; (b) the currents from lane 1 to lane 2. The black lines for $p = 0$; the red lines for $p = 0.25$; the blue lines for $p = 0.5$; the green lines for $p = 0.75$. The system parameters are: $N = 1000$, $\Omega_A = 0.6$, $\Omega_D = 0.2$, $\alpha = 0.2$, $\beta = 0.6$ and $\Omega = 5$.

that from lane 1 to lane 2. With the increase of x, the difference between the two currents becomes smaller and they are approximately the same when $x \gtrsim 0.6$ (see the right part of Fig. 3(a)).

We next investigate the effect of different values of p on density. There are two special cases: $p = 0$ and $p = 1$. When $p = 0$, it means that a particle at site $N/2$ on lane 2 cannot move forward to site $(N/2+1)$, but it can change to the other lane or detach from the site. When Ω and Ω_D are small, density at site $N/2$ on lane 2 is approximately equal to 1 (see Fig. 4(a)). Conversely, density is approximately equal to 0 at site $(N/2 + 1)$ on lane 2 (see Fig. 4(a)) when Ω and Ω_A are small. The explanation of this is that there are two ways that can lead to an appearance of a particle at site $(N/2 + 1)$ on lane 2: (i) random attachment to the site, or (ii) lane change to the site when $p = 0$. When Ω_A and Ω are very small, the probability of having a particle at this site is also very small, density on this site thus is almost equal to 0. It is also found that density on lane 2 for $x < 0.5$ is monotonically increasing when $p \leq 0.25$ and $\Omega \leq 5$ as shown in Fig. 4(a).

When $p = 1$, sites on lane 2 become homogeneous, namely, dynamics of a particle (i.e., jumping ahead, attaching and detaching, lane-changing) at site $N/2$ are completely the same as on other sites (except boundaries). In this case, the two lanes are equivalent. Density and current profiles of homogeneous two-lane TASEP coupled with Langmuir kinetics have been investigated in our recent paper [23].

When $0 < p < 1$, the effect of local inhomogeneity gradually weakens with the increase of p. When $p \geq 0.5$ the density profiles essentially remains unchanged with the further increase of p, except near $x = N/2$.

Fig. 5 shows the inter-lane currents on both the lanes for different values of p at $\Omega = 5$. In Fig. 5(a), one can see that the current from lane 2 to lane 1 decreases with the increase of p at the near left of site $N/2$, while it increases

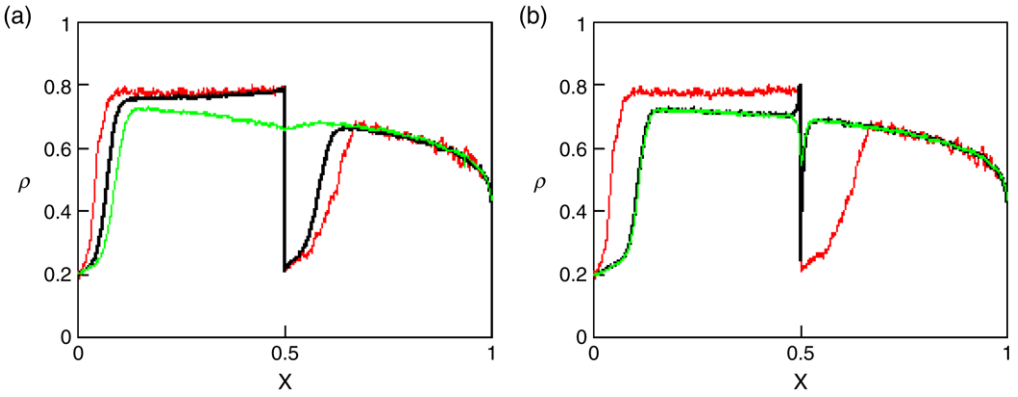

Fig. 6. (Color online) Density profiles for the single-lane PFF model with local inhomogeneity (the red line) and our two-lane model (the black line for lane 2 and green line for line 1) for $p = 0.25$. (a) $\Omega = 0.5$ and (b) $\Omega = 50$. The system parameters are: $N = 1000$, $\Omega_A = 0.6$, $\Omega_D = 0.2$, $\alpha = 0.2$ and $\beta = 0.6$.

at the right part of the system. In contrast, the current from lane 1 to lane 2 increases at the near left of site $N/2$ (see Fig. 5(b)). Nevertheless, we need to point out that at the near right of site $N/2 + 1$, the current from lane 1 to lane 2 first increases and then decreases with p, and at $0.55 \lesssim x \lesssim 0.7$, the current increases and then remains a constant with the increase of p. We believe that this intricate behavior is due to finite size effect as we have not observed this phenomena in a large system size such as $N = 10\,000$. When $p > 0.75$, it is found that the the local inhomogeneity essentially has no effect on the inter-lane currents.

Our simulations show that the density profiles obtained from our model are in quantitative agreement with that in the single-lane PFF model [5] with a local inhomogeneity [24,27]. More precisely, when Ω is small, only few particles can change to the other lane. In this case, the density profiles of lane 2 are well in agreement with that of the single-lane PFF model with local inhomogeneity (see Fig. 6(a)), that is, the single-lane PFF with local inhomogeneity is almost equivalent to lane 2 at a small value of Ω. However, with the increase of Ω, difference of densities on lane 2 and lane 1 becomes smaller and smaller, and the density profiles of lane 2 and lane 1 are lower than that of the single-lane PFF model with local inhomogeneity (see Fig. 6(b)). The decrease of density can be attributed to the effect of lane change. Further increasing Ω (e.g., $\Omega = 500$), the density profiles of the two lanes become essentially the same (not shown in Fig. 6). In this case, the effect of local inhomogeneity vanishes and the two-lane model is equivalent to the PFF model without local inhomogeneity.

Finally, we determine the average density (the average of the density of both lanes) and average currents of two lanes for different Ω under three conditions: (i) Ω_A, Ω_D and p are small, e.g., $\Omega_A = 0.03$, $\Omega_D = 0.01$, $p = 0.01$; (ii) Ω_A and Ω_D are large, but p is small, e.g., $\Omega_A = 3$, $\Omega_D = 1$, $p = 0.01$; and (iii) Ω_A and Ω_D are small, but p is large, e.g., $\Omega_A = 0.03$, $\Omega_D = 0.01$, $p = 0.5$.

In case (i), it can be seen that the change of average density profile with Ω is quite complex, especially at the left bulk (see Fig. 7(a)). The average density profile firstly enhances, and a shock wave appears ($\Omega = 0.5$). Then the shock wave gradually disappears and the density profile further enhances ($\Omega = 5$). When Ω increases from 5 to 50, the density profile lowers down marginally and it further lowers down with the increase of Ω. In contrast, the change of the average current is simple: it increases with the increase of Ω (see Fig. 7(b)).

In cases (ii) and (iii) (see Fig. 7(c)–(d)), the situation is much simpler. In case (ii), with the increase of Ω, the average currents slightly increase. The average density in the left bulk decreases for $0.2 \lesssim x < 0.5$ and essentially remains unchanged for $x < 0.2$. In the right bulk, the shock moves left with the increase of Ω. In case (iii), the average current slightly increases and the average density slightly decreases with the increase of Ω.

4. Mean-field approximation

In this section, a mean-field approximation (MFA) is developed. As shown in Ref. [6], the mean-field approximation for models of the type discussed in the present paper is valid if and only if the corresponding system with periodic boundary conditions has a factorized steady state without correlations. Our MFA is valid because factorization holds in our model since the Langmuir rates are the same for both the lanes and the coupling between the two lanes is symmetric.

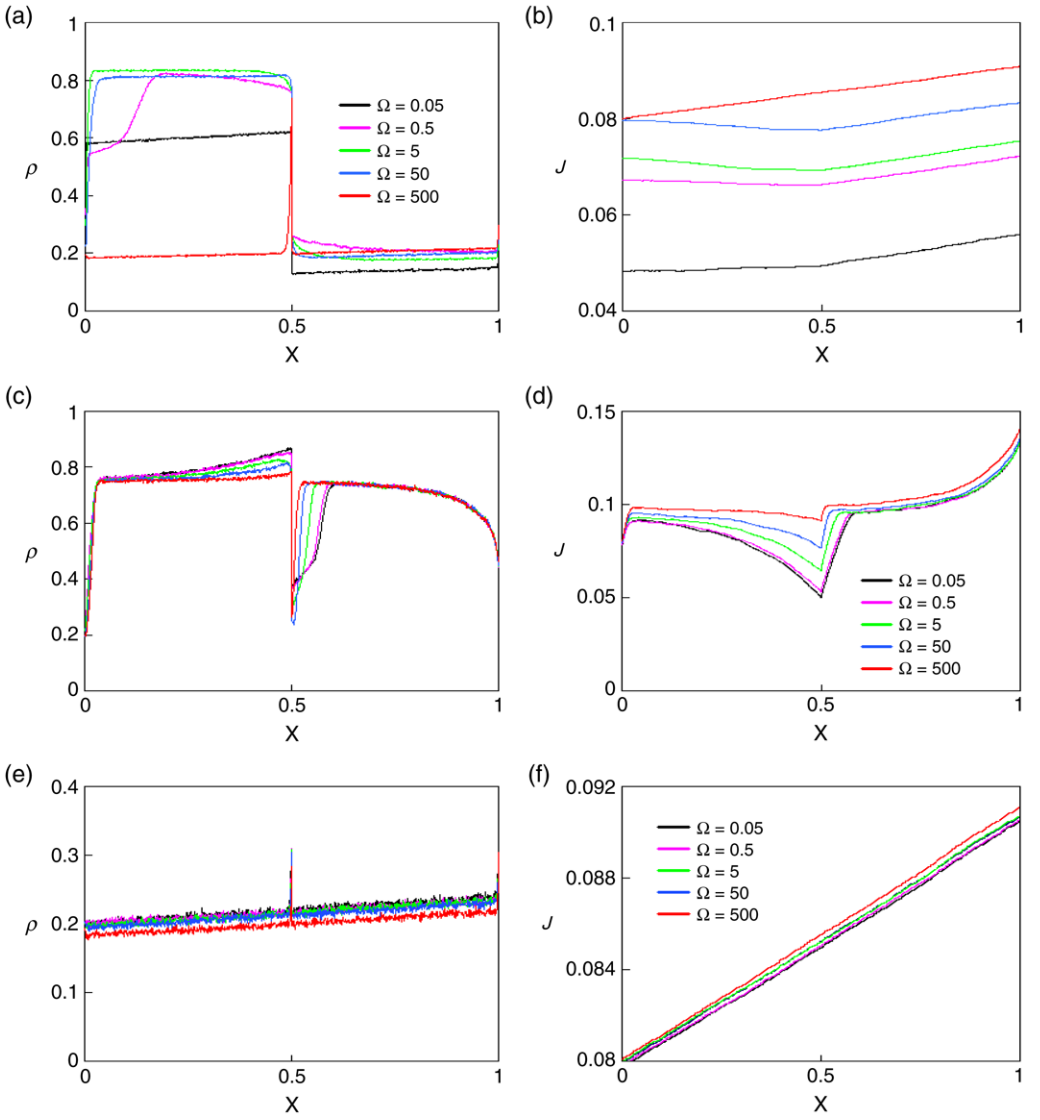

Fig. 7. (Color online) Average density and current of two lanes for different Ω. (a) and (b) $\Omega_A = 0.03$, $\Omega_D = 0.01$, $p = 0.01$; (c) and (d) $\Omega_A = 3$, $\Omega_D = 1$, $p = 0.01$; and (e) and (f) $\Omega_A = 0.03$, $\Omega_D = 0.01$, $p = 0.5$. The system parameters are: $N = 1,000$, $\alpha = 0.2$ and $\beta = 0.6$.

A one-lane system of size N with a local inhomogeneity can be divided into two one-lane subsystems with size $N/2$ each connected by the inhomogeneous site. This approach has been widely adopted and used in Refs. [25–27]. Our MFA is developed based on the concepts of effective injection and ejection rates proposed in [25]. Following this approach, the left subsystem in the ℓth lane is a homogeneous TASEP with injection rate α at site 1 and ejection rate $\beta_{\ell,\mathrm{eff}}$ at site $N/2$ ($\ell = 1$ or 2). There are three ways to exit site $N/2$: (i) detaching from the site with rate w_D, (ii) changing to the other lane with rate w, and (iii) jumping to site $(N/2+1)$. Thus, the effective ejection rates $\beta_{2,\mathrm{eff}}$ and $\beta_{1,\mathrm{eff}}$ on lanes 2 and 1 can be written as:

$$\beta_{2,\mathrm{eff}} = \omega_D + p(1-\rho_{2,N/2+1}) + \omega\rho_{2,N/2+1}(1-\rho_{1,N/2}), \tag{1}$$

$$\beta_{1,\mathrm{eff}} = \omega_D + 1 - \rho_{1,N/2+1} + \omega\rho_{1,N/2+1}(1-\rho_{2,N/2}). \tag{2}$$

While at the boundaries of the left subsystem one obtains:

$$\rho_{\ell,1} = \alpha, \qquad \rho_{\ell,N/2} = 1 - \beta_{\ell,\mathrm{eff}}. \tag{3}$$

Similarly, the right subsystems are homogeneous TASEPs with injection rates $\alpha_{\ell,\mathrm{eff}}$ at site $(N/2+1)$ and ejection rate β at site N. The entrance at site $(N/2+1)$ has three ways: attaching to the site with rate w_A, changing to the site from the other lane with rate w, and jumping to the site from site $N/2$ of the same lane. Thus, the effective injection rate $\alpha_{\ell,\mathrm{eff}}$ can be written as:

$$\alpha_{2,\mathrm{eff}} = \omega_A + p\rho_{2,N/2} + \omega\rho_{1,N/2+2}(1-\rho_{2,N/2+1}), \tag{4}$$

$$\alpha_{1,\mathrm{eff}} = \omega_A + \rho_{1,N/2} + \omega\rho_{2,N/2+2}(1-\rho_{1,N/2+1}), \tag{5}$$

while at the boundaries of the right subsystems one obtains:

$$\rho_{\ell,N} = 1-\beta, \qquad \rho_{\ell,N/2+1} = \alpha_{\ell,\mathrm{eff}}, \qquad \rho_{\ell,(N/2+2)} \approx \rho_{\ell,(N/2+1)}. \tag{6}$$

Substituting Eqs. (3) and (6) into Eqs. (1) and (2), (4) and (5), we obtain:

$$\beta_{2,\mathrm{eff}} = \omega_D + p(1-\alpha_{2,\mathrm{eff}}) + \omega\alpha_{2,\mathrm{eff}}\beta_{1,\mathrm{eff}}, \tag{7}$$

$$\beta_{1,\mathrm{eff}} = \omega_D + 1 - \alpha_{1,\mathrm{eff}} + \omega\alpha_{1,\mathrm{eff}}\beta_{2,\mathrm{eff}}, \tag{8}$$

$$\alpha_{2,\mathrm{eff}} = \omega_A + p(1-\beta_{2,\mathrm{eff}}) + \omega\alpha_{1,\mathrm{eff}}(1-\alpha_{2,\mathrm{eff}}), \tag{9}$$

$$\alpha_{1,\mathrm{eff}} = \omega_A + 1 - \beta_{1,\mathrm{eff}} + \omega\alpha_{2,\mathrm{eff}}(1-\alpha_{1,\mathrm{eff}}). \tag{10}$$

Eqs. (7)–(10) are nonlinear equations with four unknowns. These can be solved numerically. For instance, when $\Omega = 0.5$, $p = 0.25$, $\Omega_A = 0.6$ and $\Omega_D = 0.2$, we obtain $\beta_{2,\mathrm{eff}} = 0.201143$, $\beta_{1,\mathrm{eff}} = 0.340432$, $\alpha_{2,\mathrm{eff}} = 0.200306$ and $\alpha_{1,\mathrm{eff}} = 0.657565$. When $\Omega = 5$, $p = 0.25$, $\Omega_A = 0.6$ and $\Omega_D = 0.2$, we obtain $\beta_{2,\mathrm{eff}} = 0.200375$, $\beta_{1,\mathrm{eff}} = 0.340432$, $\alpha_{2,\mathrm{eff}} = 0.199953$ and $\alpha_{1,\mathrm{eff}} = 0.5798$. Thus, the boundary conditions for the four subsystems, i.e., densities at site $N/2$ and $(N/2+1)$, can be determined explicitly.

We next analyze the density profiles in the bulks of the four subsystems. The occupation variable $(\tau_{\ell,i})$ is represented as the state of the ith site in the ℓth lane. $\tau_{\ell,i} = 1$ or 0 corresponds to the site being occupied or empty. The corresponding equation for the evolution of particle densities $\langle\tau_{\ell,i}\rangle$ in a bulk (i.e., $1 < i < N/2$, or $(N/2+1) < i < N$), say on lane 1, can be written as

$$\begin{aligned}\frac{\mathrm{d}\langle\tau_{1,i}\rangle}{\mathrm{d}t} &= \langle\tau_{1,i-1}(1-\tau_{1,i})\rangle - \langle\tau_{1,i}(1-\tau_{1,i+1})\rangle + \omega\langle\tau_{2,i}\tau_{2,i+1}(1-\tau_{1,i})\rangle - \omega\langle\tau_{1,i}\tau_{1,i+1}(1-\tau_{2,i})\rangle \\ &\quad + \omega_A\langle 1-\tau_{1,i}\rangle - \omega_D\langle\tau_{1,i}\rangle,\end{aligned} \tag{11}$$

where $\langle\cdots\rangle$ denotes a statistical average. The term $\omega\langle\tau_{1,i}\tau_{1,i+1}(1-\tau_{2,i})\rangle$ is the average current from site i in lane 1 to site i in lane 2. The first two terms in Eq. (11) correspond to particle movement; the middle two terms correspond to particle lane changing, and the last two terms correspond to attachment and detachment of particles. When N is large, i.e., $N \gg 1$, we can transfer the coarse-grained stationary-state Eq. (11) to continuum mean-field approximation. We replace $\langle\tau_{1,i}\rangle$ and $\langle\tau_{1,i+1}\rangle$ with $\rho_{1,i}$ and $\rho_{1,i+1}$, then set

$$\rho_{1,i\pm1} = \rho(x) \pm \frac{1}{N}\frac{\partial\rho}{\partial x} + \frac{1}{2N^2}\frac{\partial^2\rho}{\partial x^2} + O\left(\frac{1}{N^3}\right). \tag{12}$$

Substituting Eq. (12) into Eq. (11), we obtain:

$$\frac{\partial\rho_1}{\partial t'} = \frac{1}{2N}\frac{\partial^2\rho_1}{\partial x^2} + (2\rho_1-1)\frac{\partial\rho_1}{\partial x} + \Omega_A(1-\rho_1) - \Omega_D\rho_1 - \Omega(1-\rho_2)\rho_1^2 + \Omega\rho_2^2(1-\rho_1), \tag{13}$$

where $t' = t/N$, $\Omega = \omega N$, $\Omega_A = \omega_A N$ and $\Omega_D = \omega_D N$.

Similarly, we have:

$$\frac{\partial\rho_2}{\partial t'} = \frac{1}{2N}\frac{\partial^2\rho_2}{\partial x^2} + (2\rho_2-1)\frac{\partial\rho_2}{\partial x} + \Omega_A(1-\rho_2) - \Omega_D\rho_2 - \Omega(1-\rho_1)\rho_2^2 + \Omega\rho_1^2(1-\rho_2). \tag{14}$$

Eqs. (13) and (14) can also be solved using numerical methods. The numerical solution is obtained by Newton iteration, and the simulation results are used as initial conditions. These numerical results are shown in Fig. 8, which are in agreement with our Monte Carlo simulations.

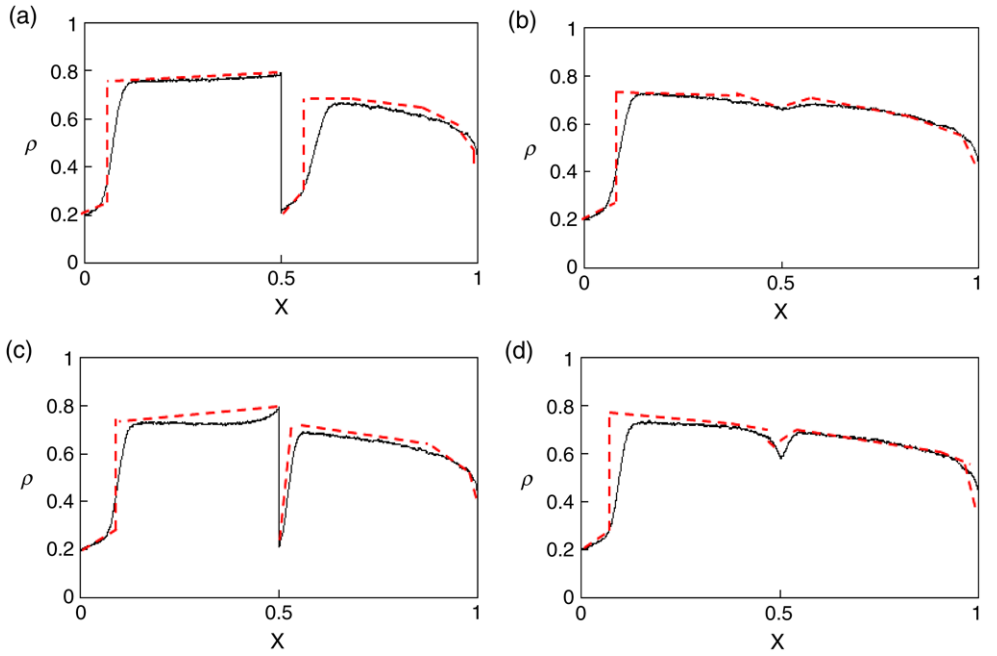

Fig. 8. (Color online) Density profiles $\rho(x)$ for different values of Ω on both lanes at $p = 0.25$. (a) and (c) for lane 2; (b) and (d) for lane 1. (a) and (b) for $\Omega = 0.5$; (c) and (d) for $\Omega = 5$. Red lines for mean-field approximation and black lines for Monte Carlo simulations. The system parameters are: $N = 1000$, $\Omega_A = 0.6$, $\Omega_D = 0.2$, $\alpha = 0.2$ and $\beta = 0.6$.

5. Conclusion

This paper investigated the effects of local inhomogeneity in two-lane asymmetric simple exclusion processes coupled with Langmuir kinetics (LK) using Monte Carlo simulations (MCS) and mean-field approximation (MFA). The results of the Monte Carlo simulations agree well with the results of mean-field approximation. The model is related to some biological processes such as the movement of molecular motors on parallel homogeneous and inhomogeneous filaments without restrictions for them to jump between these filaments. Also, related to that protein motors can randomly attach to or detach from the filaments. The local inhomogeneity is only assumed to locate at the middle site on one of the two lanes.

The system mainly demonstrates the following complex behavior on the two lanes: (i) The local inhomogeneity has strong effects on both the lanes when the hopping rate at the local inhomogeneity, p, is small and the lane-changing rate Ω is not so small; with the increase of hopping rate p, the local inhomogeneity effects are weakened; (ii) With the increase of lane-changing rate Ω, the local inhomogeneity effects are also weakened; (iii) The inter-lane currents are different and such differences will gradually decrease when increasing either p and/or Ω; (iv) When Ω_A, Ω_D and p are small, the average density profile exhibits a complex variation behavior with the increase of Ω.

Acknowledgements

R. Wang acknowledges the support of the ASIA:NZ Foundation Higher Education Exchange Program (2005), the Massey University Research Fund (2007), and the Massey University International Visitor Research Fund (2007). R. Jiang acknowledges the support of the National Basic Research Program of China (2006CB 705500), the National Natural Science Foundation of China (NNSFC) under Key Project No. 10532060, Project Nos. 10404025, 10672160 and 70601026, and the CAS Special Foundation. We are grateful to Michele Wagner for proofreading this manuscript. The authors gratefully acknowledge the comments and suggestions of the anonymous reviewers, which helped in improving the clarity and the quality of the paper.

References

[1] M. Schliwa, G. Woehlke, Nature 422 (2003) 759 and references therein.
[2] J. Krug, Phys. Rev. Lett. 67 (1991) 1882.

[3] B. Derrida, Phys. Rep. 301 (1998) 65.
[4] G.M. Schütz, in: C. Domb, J.L. Lebowitz (Eds.), Phase Transitions and Critical Phenomena, vol. 19, Academic Press, San Diego, 2001.
[5] A. Parmeggiani, T. Franosch, E. Frey, Phys. Rev. Lett. 90 (2003) 086601;
A. Parmeggiani, T. Franosch, E. Frey, Phys. Rev. E 70 (2004) 046101.
[6] V. Popkov, A. Rákos, R.D. Willmann, A.B. Kolomeisky, G.M. Schütz, Phys. Rev. E 67 (2003) 066117.
[7] S. Katz, J.L. Lebowitz, H. Spohn, J. Stat. Phys. 34 (1984) 497.
[8] B. Schmittmann, R.K.P. Zia, in: C. Domb, J. Lebowitz (Eds.), Phase Transitions and Critical Phenomena, vol. 17, Academic Press, London, 1995.
[9] J.T. MacDonald, J.H. Gibbs, A.C. Pipkin, Biopolymers 6 (1968) 1.
[10] R. Lipowsky, S. Klumpp, T. Nieuwenhuizen, Phys. Rev. Lett. 87 (2001) 108101;
S. Klumpp, R. Lipowsky, J. Stat. Phys. 113 (2003) 233.
[11] K. Kruse, K. Sekimoto, Phys. Rev. E 66 (2002) 031904.
[12] G. Lakatos, T. Chou, J. Phys. A 36 (2003) 2027.
[13] L.B. Shaw, R.K.P. Zia, K.H. Lee, Phys. Rev. E 68 (2003) 021910.
[14] T. Chou, Biophys. J. 85 (2003) 755.
[15] K. Nishinari, Y. Okada, A. Schadschneider, D. Chowdhury, Phys.Rev. Lett. 95 (2005) 118101.
[16] J. Howard, Mechanism of Motor Proteins and the Cytoskeleton, Sinauer Associates, Sunderland, MA, 2001.
[17] Y. Okada, N. Hirokawa, Science 283 (1999) 1152.
[18] E. Pronina, A.B. Kolomeisky, J. Phys. A 37 (2004) 9907.
[19] E. Pronina, A.B. Kolomeisky, Physica A 372 (2006) 12; J. Stat. Mech. (2005) P07010.
[20] T. Mitsudo, H. Hayakawa, J. Phys. A 38 (2005) 3087.
[21] T. Reichenbach, T. Franosch, E. Frey, Phys. Rev. Lett. 97 (5) (2006) 050603.
[22] R. Jiang, R. Wang, Q.S. Wu, Physica A 375 (1) (2007) 247.
[23] R. Wang, R. Jiang, M. Liu, J. Liu, Q.S. Wu, Internat. J. Modern. Phys. C 18 (9) (2007).
[24] P. Pierobon, M. Mobilia, R. Kouyos, E. Frey, Phys. Rev. E 74 (3) (2006) 031906.
[25] A.B. Kolomeisky, J. Phys. A 31 (1998) 1153.
[26] L.B. Shaw, A.B. Kolomeisky, K.H. Lee, J. Phys. A 37 (2004) 2105.
[27] K. Qiu, X.-Q. Yang, W. Zhang, D. Sun, Y. Zhao, Physica A 373 (2007) 1;
X.-Q. Yang, K. Qiu, W. Zhang, L. Ren, W. Xu, Y.-J. Deng, Physica A 379 (2) (2007) 595.
[28] T. Chou, G. Lakatos, Phys. Rev. lett. 93 (19) (2004) 198101;
G. Lakatos, T. Chou, A.B. Kolomeisky, Phys. Rev. E 71 (1) (2005) 011103;
G. Lakatos, J. O'Brien, T. Chou, J. Phys A 39 (10) (2006) 2253.
[29] B. Trpisová, J.A. Tuszynski, Phys. Rev. E 55 (3) (1997) 3288.
[30] S. Huang, D.E. Ingber, Nature Cell Biol. 1 (1999) E131.
[31] K. Kullander, TINS 28 (55) (2005) 239.
[32] B. Estrella, et al., Environ. Health Perspect 113 (2005) 607.
[33] A. Alberts, et al., The Molecular Biology of the Cell, Garland, New York, 1994.